Observation of Picometer Vertical Emittance with a Vertical Undulator

K. P. Wootton,[1,*] M. J. Boland,[1,2] R. Dowd,[2] Y.-R. E. Tan,[2] B. C. C. Cowie,[2] Y. Papaphilippou,[3] G. N. Taylor,[1] and R. P. Rassool[1]

[1]*School of Physics, The University of Melbourne, Melbourne VIC 3010, Australia*
[2]*Australian Synchrotron, 800 Blackburn Road, Clayton VIC 3168, Australia*
[3]*European Organization for Nuclear Research (CERN), BE Department, 1211 Geneva 23, Switzerland*

(Received 11 July 2012; published 8 November 2012)

Using a vertical undulator, picometer vertical electron beam emittances have been observed at the Australian Synchrotron storage ring. An APPLE-II type undulator was phased to produce a horizontal magnetic field, which creates a synchrotron radiation field that is very sensitive to the vertical electron beam emittance. The measured ratios of undulator spectral peak heights are evaluated by fitting to simulations of the apparatus. With this apparatus immediately available at most existing electron and positron storage rings, we find this to be an appropriate and novel vertical emittance diagnostic.

DOI: 10.1103/PhysRevLett.109.194801 PACS numbers: 29.27.−a, 41.60.−m, 41.75.Ht, 41.85.Lc

In recent years, storage ring light sources and damping rings have produced electron and positron beams of diminishing vertical size [1–3]. Beams of unprecedented small size are demanded particularly for electron-positron colliders at both the energy [4] and intensity frontiers [5]. With vertical dimensions of several μm, direct measurement of beam size is approaching diffraction limits of visible light and hard x-ray diagnostics [6]. We report on the development of a new vertical electron beam size measurement technique which utilizes a vertical undulator. Vertical undulators are rare [7]—typically beams are deflected in the horizontal plane. In this work, an elliptically polarized undulator was phased as a vertical undulator. We present direct observation of μm vertical beam sizes corresponding to picometer radian (pm rad) vertical beam emittances, and remark that this technique is immediately achievable using existing photon beam lines of electron storage ring light sources.

The spectral and angular profile of undulator radiation is especially sensitive to the transverse emittance [8], defined as an envelope in position-angle phase space of the electron beam ensemble. Projections of the angular profile of undulator harmonics can be used to characterize the beam emittance. This has been demonstrated using a soft x-ray undulator producing a vertical field [9], referred to as a horizontal undulator because the beam is deflected in that transverse direction.

Previous analytical descriptions and modeling of undulator brilliance focused on determination of the absolute photon beam brilliance [8], and identified the brilliance of even harmonics as especially sensitive to the transverse emittance [10], using a horizontal undulator. The absolute photon beam brilliance is a difficult quantity to measure. A novel technique has been previously proposed, measuring the ratio of intensities of the first and second undulator harmonics and comparing with simulations of photon brilliance [11,12]. We present measurements of the stored electron beam size by expanding this idea and taking the ratios of many adjacent pairs of odd and even harmonics.

This technique shares similarities with another projection measurement of vertical emittance [1,13] but differs by passing, as opposed to masking, the on-axis null radiation field. Illustrated in Fig. 1 are simulated transverse profiles of the intensity of undulator radiation. Instead of trying to measure the absolute photon flux of the on-axis null field of the even harmonics, F_{n-1}, we calibrate this low flux against the high-flux peaks of the odd harmonics passing the same aperture, F_n. The ratio of fluxes of

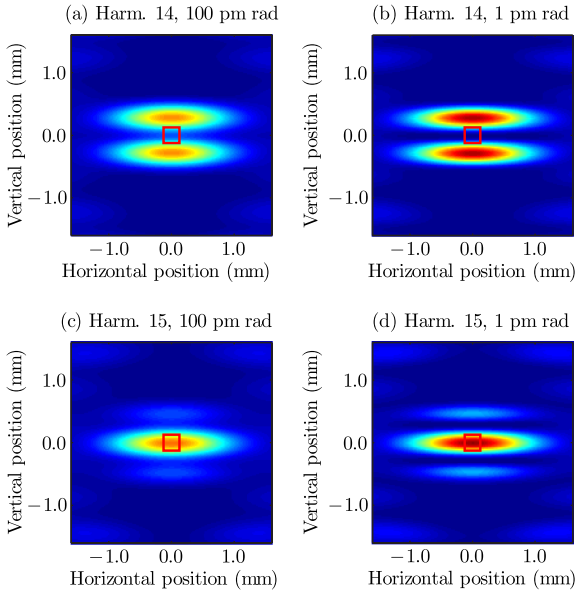

FIG. 1 (color online). SPECTRA [22] simulation of profile of undulator radiation 15 m from the undulator center, with the 250×250 μm rectangular pinhole aperture outline marked in red. (a) Harmonic 14, 100 pm emittance. (b) Harmonic 14, 1 pm emittance. (c) Harmonic 15, 100 pm emittance. (d) Harmonic 15, 1 pm emittance.

TABLE I. Electron beam and undulator properties used in simulation.

	Parameter	Value	Units
	Beam		
E_0	Energy	3.0	GeV
σ_E	Energy spread	0.11	%
ε_x	Horizontal emittance	10	nm rad
	Undulator		
λ_u	Period length	75	mm
B_u	Peak field	0.55	T
K_u	Deflection parameter	3.8	...
N_u	Number of full periods	25	...

adjacent undulator harmonics F_{n-1}/F_n is evaluated. For Fig. 1, the ratio of flux passing for the even 14th to odd 15th harmonics is $F_{n-1}/F_n = 0.42$ for a beam of 100 pm rad geometric vertical emittance shown in (a) and (c), and 0.17 for 1 pm rad shown in (b) and (d).

The undulator used was an Advanced Planar Polarized Light Emitter (APPLE-II) type undulator [14,15]. Properties of the electron beam and undulator are summarized in Table I below. The magnetic arrays of the undulator were phased to produce a horizontal field, deflecting the electron beam in the vertical plane. A gap of 17.1 mm was selected—close to the minimum gap—producing a peak horizontal field of 0.55 T. Magnetic measurements of the undulator during acceptance demonstrate that in the configuration for vertical polarization at minimum gap, the axis of the undulator field is within -6 ± 30 mrad of the nominal horizontal orientation [15].

Vertical emittance growth due to undulator self-dispersion was calculated [16], for the stated undulator and the normal Australian Synchrotron user lattice with 0.1 m distributed horizontal dispersion in the insertion straights. For a device of 2 m length, we calculate an emittance increase due to vertical self-dispersion of $\Delta\epsilon_y = 0.012$ pm rad, which is well below the lowest achieved vertical emittance in this ring of $\epsilon_y \approx 1$–2 pm rad [2], and indeed below the quantum limit of vertical emittance.

The APPLE-II undulator serves the soft x-ray user beam line of the Australian Synchrotron [17]. After closing the undulator to its operating gap, the storage ring skew quadrupoles were optimized for a range of emittance configurations using the linear optics from closed orbits (LOCO) routine [18]. The measured undulator spectra are presented in Fig. 2 for vertical emittances from 2.6 ± 1.1 pm rad in blue up to 1750 ± 330 pm rad in red.

We measure the photon flux passing an on-axis pinhole. The pinhole used is four blades of the white-beam slits, closed to form a rectangular pinhole aperture of approximately 250×250 μm. We choose an aperture which is small in both the horizontal and vertical dimensions, to minimize any contribution from the horizontal emittance. At a distance of 15.0 m from the undulator center, it passes undulator radiation within an opening angle of $\theta = 1.7 \times 10^{-5}$ rad.

Undulator measures of emittance typically assume the weak undulator limit $K_u \leq 1$, producing beams within a central cone of radius $\theta_{\max} \approx 0.3(K_u/\gamma)$ [10]. In the strong undulator limit $K_u > 1$, the cone approximation breaks down. With odd harmonic number $n > 3$ and $n \geq (N_u/3)$, the half angle of the first interference minima is given by [19,20]

$$\theta_{\max} = \frac{K_u}{\gamma}\frac{\pi}{2n}\frac{(1 + K_u^2/2)}{(1 + 2K_u^2)}. \quad (1)$$

Using Eq. (1) for $n = 15$ and parameters of Table I, we place an upper limit on the pinhole half angle radius of $\theta_{\max} = 0.029(K_u/\gamma)$. This corresponds in Fig. 3 to the maximum in ratio F_{14}/F_{15} for pinhole offset, and pinhole half-apertures greater than this exhibiting no sensitivity to vertical emittance. The ratio of fluxes is optimized by minimizing the vertical offset of the pinhole. This is achieved experimentally by scanning the pinhole vertically through the interference pattern for the unambiguous

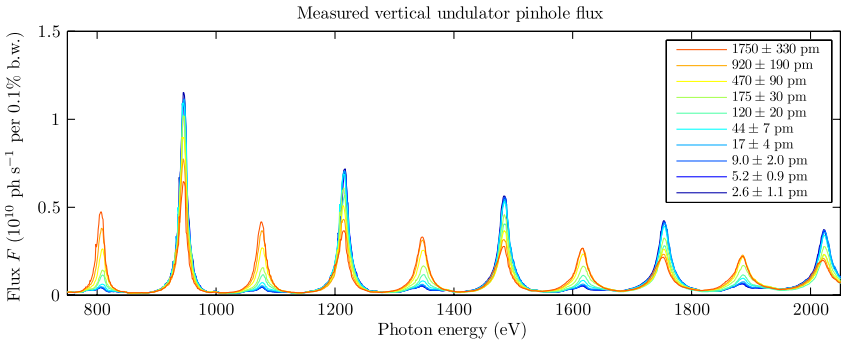

FIG. 2 (color online). Measured undulator spectra for vertical emittances calibrated with LOCO, from minimum in blue up to maximum in red. Shown in order of increasing photon energy are undulator harmonics 6–15. Small vertical emittances (blue) exhibit lowest intensity at even harmonics and highest intensity at odd harmonics. High vertical emittances (red) exhibit equal intensities at both even and odd harmonics.

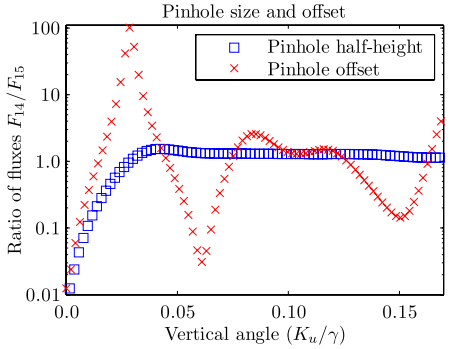

FIG. 3 (color online). Flux ratio dependence for vertical emittance 0 pm rad, harmonics 14 and 15, and beam parameters of Table I. A centered pinhole of half-height is illustrated in blue, and vertical offset of a pinhole of 50 μm in red. An angle of $0.10(K_u/\gamma) \equiv 1.0$ mm vertical position at 15 m, cf. Figs. 1(b) and 1(d).

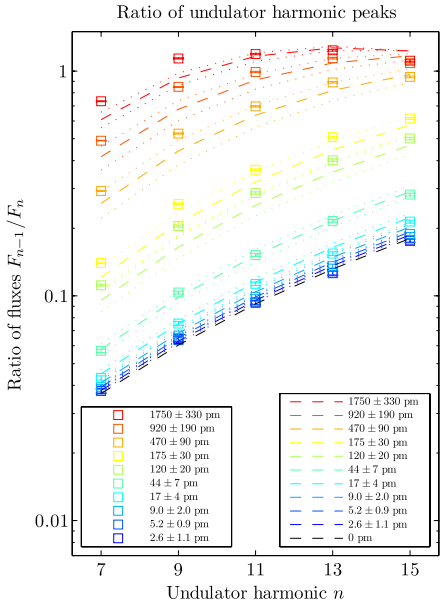

FIG. 4 (color online). Model 261×261 μm pinhole fitted to experimental data. Measured undulator peaks marked as squares, fitted SPECTRA simulations denoted by dashed contours increasing from lower flux ratios corresponding to lower emittances in blue, up to higher flux ratios in red. The simulated contour of a beam with zero vertical emittance is shown in black. Uncertainties of measured ratios shown as error bars, and dotted contours for fitted model.

intensity maximum of an odd undulator harmonic, as illustrated in Fig. 1(d).

The existing beam line optics were used for the spectrometer. The beam line employs a linear grating for the monochromator, and several gold-coated toroidal mirrors to focus the beam. The M absorption edges of the gold coatings restrict our studies to photon energies below 2200 eV. The spectrometer grating and all focussing mirrors are positioned downstream of the aperture. A second aperture was used to select a single grating diffraction order. Background was subtracted by measuring the photon flux with the undulator open to its maximum gap. The drain current of a silicon photodiode was detected, from which photon flux was calculated [21]. We calculate and present the photon flux on an absolute scale in Fig. 2; however, in the evaluation of the ratio arbitrary units would suffice.

Using the SPECTRA code [22], the flux of monochromated undulator radiation passing a pinhole was simulated. The dimensions of the pinhole used in measurements were not available due to inaccuracies in motor lash. To extract these dimensions from our data, we fit a single free parameter using all data sets simultaneously—the vertical dimension of the pinhole. Envelopes of beam emittance corresponding to LOCO measurements were fitted to the measured peak ratios, minimizing the χ^2 test statistic. These ratios of F_{n-1}/F_n harmonics are presented in Fig. 4. The χ^2 test statistic is minimized for a pinhole of 261×261 μm. We have chosen to fit emittance contours based on global LOCO emittances; however, this emittance monitor is intrinsically local to one point in the ring. Hence the apparent emittance measured may vary from the global projected emittance [23], for some contours of Fig. 4.

Uncertainties are presented in Fig. 4 corresponding to both the measured undulator spectra and fitted emittance envelopes. The fitted envelopes and uncertainties correspond to the beam emittance evaluated using LOCO. Uncertainties in measured ratios were evaluated from scans of the background flux with the undulator open to its maximum gap, nominally bending magnet edge radiation. This was measured more than an order of magnitude lower than the minimum undulator flux.

The major finding of this work is that the ratios of undulator pinhole flux can be used to measure vertical emittance. A vertical undulator appears to be an appropriate vertical emittance diagnostic in storage rings attempting to achieve lowest vertical emittance.

It is suggested in literature that such a technique should be possible for the measurement of horizontal emittance [11], but no published measurements have been found. It is also suggested that F_{n-1}/F_n should tend to zero for beams of zero transverse emittance [11]. Shown in Fig. 4 are envelopes of measured and simulated emittance ratios, including the envelope for zero vertical electron beam emittance. This envelope highlights the distinction between electron beam size and the size of the photon source, which in the limit of zero electron beam size is defined by the amplitude of undulator oscillations. The photon beam source size measured using this ratio technique is the convolution of the rms undulator deflection with the electron beam transverse dimension [24].

Advantages of the technique are the ability to exploit the linearity in detector response over a photon energy range spanning keV, and decades of intensity. The measurement of a ratio—as opposed to absolute photon beam

brilliance—absolves of the need for measurement of photon flux on an absolute scale.

The major uncertainty in the technique is the pinhole dimension. Future experiments to measure the vertical emittance should consider using a pinhole of known diameter. We fitted all spectra with a single free parameter being the pinhole dimension; however, with this fixed the free parameter becomes the electron beam size. The dependence of the flux ratio upon pinhole vertical offset and size is illustrated in Fig. 3 for a beam of 0 pm rad vertical emittance.

The effect of energy spread on peak width has previously been quantified [11,25]. In simulation, we consider the effect of energy spread on peak height. Increasing the relative energy spread by 25%, we find that the measured peak height ratio does not exceed uncertainties in the measured peak ratios for beams with vertical emittance less than 200 pm rad (approximately 2% emittance ratio). The energy spread can be constrained within an uncertainty of 11% from measurements of the bunch length σ_t,

$$\sigma_t = 2\pi f_s |\gamma^{-2} - \alpha_c| \sigma_E. \quad (2)$$

The momentum compaction factor α_c and synchrotron frequency f_s can both be measured within 2% uncertainty using resonant spin depolarization [26] and a spectrum analyzer, respectively. The bunch length can be measured within 7% uncertainty using a calibrated streak camera and removing chromatic effects [27] with a band pass filter. Hence uncertainty in electron beam energy spread should not limit the application of this technique.

Closing an undulator in the vertical direction has the effect of increasing the vertical dispersion of the electron beam. Our calculations, following [16], show that the increase is orders of magnitude lower than the quantum limit. It would be interesting to consider using the vertical undulator as a vertical emittance damping wiggler.

In conclusion, the observation of pm rad vertical emittance electron beams has been demonstrated using a vertical undulator. The difference between pm rad vertical emittance beams is resolvable using this technique. Exploiting a precision photon beam line, the measured ratios of on-axis pinhole flux agree closely with simulations. With a pinhole of fixed diameter, this technique should yield quantitative measurements of the electron beam vertical emittance.

This research was undertaken using the soft x-ray beam line and storage ring at the Australian Synchrotron, Victoria, Australia.

*k.wootton@student.unimelb.edu.au

[1] M. Aiba, M. Böge, N. Milas, and A. Streun, Nucl. Instrum. Methods Phys. Res., Sect. A **694**, 133 (2012).
[2] R. Dowd, M. Boland, G. LeBlanc, and Y.-R. E. Tan, Phys. Rev. ST Accel. Beams **14**, 012804 (2011).
[3] Y. Honda, *et al.*, Phys. Rev. Lett. **92**, 054802 (2004).
[4] Editorial, Nature (London) **456**, 422 (2008).
[5] A. Cho, Science **321**, 34 (2008).
[6] J. Flanagan, in *Proceedings of International Particle Accelerator Conference 2011* (JACoW, San Sebastian, Spain, 2011), p. WEYB01.
[7] T. Tanaka, X.-M. Maréchal, T. Hara, T. Tanabe, and H. Kitamura, J. Synchrotron Radiat. **5**, 414 (1998).
[8] G. Dattoli, G. K. Voykov, and M. Carpanese, Phys. Rev. E **52**, 6809 (1995).
[9] T. Moreno, E. Otero, and P. Ohresser, J. Synchrotron Radiat. **19**, 179 (2012).
[10] G. Dattoli and G. Voykov, Nuovo Cimento B **111**, 743 (1996).
[11] M. Bakeman, W. Leemans, K. Nakamura, K. Robinson, C. Schroeder, and C. Toth, in *Proceedings of Particle Accelerator Conference 2009* (JACoW, Vancouver, BC, Canada, 2009), p. WE6RFP074.
[12] M. Bakeman, E. Esarey, W. P. Leemans, K. Nakamura, J. Osterhoff, K. Robinson, C. B. Schroeder, J. van Tilborg, C. Toth, F. Gruner, and R. Weingartner, in *Proceedings of Particle Accelerator Conference 2011* (JACoW, New York, NY, USA, 2011), p. MOP161.
[13] Å. Andersson, M. Böge, A. Lüdeke, V. Schlott, and A. Streun, Nucl. Instrum. Methods Phys. Res., Sect. A **591**, 437 (2008).
[14] S. Sasaki, Nucl. Instrum. Methods Phys. Res., Sect. A **347**, 83 (1994).
[15] C. Ostenfeld, F. Bødker, M. Pedersen, E. Christensen, M. Bøttcher, and H. Bach, in *Proceedings of Particle Accelerator Conference 2007* (JACoW, Albuquerque, New Mexico, USA, 2007), p. TUPMN006.
[16] H. Wiedemann, Nucl. Instrum. Methods Phys. Res., Sect. A **266**, 24 (1988).
[17] B. C. Cowie, A. Tadich, and L. Thomsen, AIP Conf. Proc. **1234**, 307 (2010).
[18] J. Safranek, Nucl. Instrum. Methods Phys. Res., Sect. A **388**, 27 (1997).
[19] C. Leubner and P. Torggler, Opt. Commun. **48**, 362 (1984).
[20] R. Walker, Nucl. Instrum. Methods Phys. Res., Sect. A **335**, 328 (1993).
[21] M. Krumrey, L. Büermann, M. Hoffmann, P. Müller, F. Scholze, G. Ulm, and T. Warwick, AIP Conf. Proc. **705**, 861 (2004).
[22] T. Tanaka and H. Kitamura, J. Synchrotron Radiat. **8**, 1221 (2001).
[23] A. Franchi, L. Farvacque, J. Chavanne, F. Ewald, B. Nash, K. Scheidt, and R. Tomás, Phys. Rev. ST Accel. Beams **14**, 034002 (2011).
[24] K.-J. Kim, AIP Conf. Proc. **184**, 565 (1989).
[25] J. G. Gallacher, *et al.*, Phys. Plasmas **16**, 093102 (2009).
[26] H. Panopoulos, K. Wootton, M. Boland, and R. Rassool, in *Proceedings of International Particle Accelerator Conference 2011* (JACoW, San Sebastian, Spain, 2011), p. TUPC062.
[27] T. Obina and T. Mitsuhashi, in *Proceedings of Diagnostics and Instrumentation for Particle Accelerators 2007* (JACoW, Venice, Italy, 2007), p. WEPB12.